

Cosmic ray driven dynamo in barred and ringed galaxies

K. Kulpa-Dybel¹, K. Otmianowska-Mazur¹, B. Kulesza-Żydzik¹
G. Kowal^{1,2}, D. Wóltański³, M. Hanasz³ and K. Kowalik³

¹Astronomical Observatory, Jagiellonian University, ul. Orła 171, 30-244 Kraków, Poland

²Núcleo de Astrofísica Teórica, Universidade Cruzeiro do Sul-Rua Galvão Bueno 868, CEP 01506-000 São Paulo, Brazil

³Centre for Astronomy, Nicholas Copernicus University, PL-87148 Piwnice/Toruń Poland

Abstract. We study the global evolution of the magnetic field and interstellar medium (ISM) of the barred and ringed galaxies in the presence of non-axisymmetric components of the potential, i.e. the bar and/or the oval perturbations. The magnetohydrodynamical dynamo is driven by cosmic rays (CR), which are continuously supplied to the disk by supernova (SN) remnants. Additionally, weak, dipolar and randomly oriented magnetic field is injected to the galactic disk during SN explosions. To compare our results directly with the observed properties of galaxies we construct realistic maps of high-frequency polarized radio emission. The main result is that CR driven dynamo can amplify weak magnetic fields up to few μG within few Gyr in barred and ringed galaxies. What is more, the modelled magnetic field configuration resembles maps of the polarized intensity observed in barred and ringed galaxies.

Keywords. galaxies: evolution, magnetic fields, ISM: cosmic rays, methods: numerical

1. Introduction

To explain the observational properties of the magnetic field in barred and ringed galaxies the dynamo action is necessary. It is thought that the CR driven dynamo can be responsible for the following effects: amplification of galactic magnetic fields up to several μG within a lifetime of a few Gyr; large magnetic pitch angles of about -35° ; symmetry (even, odd); maintenance of the created magnetic fields in a steady state; magnetic field which does not follow the gas distribution, i.e. magnetic fields in NGC 4736 crossing the inner gaseous ring without any change of their direction (Chyży & Buta 2008) or magnetic arms in NGC 1365 which are located between gaseous spiral (Beck et al. 2002).

2. Cosmic ray driven dynamo

CR driven dynamo is based on the following effects (details see Hanasz et al 2009 and references therein, and Hanasz et al, this volume): The CR component described by We numerically investigated the CR driven dynamo model in a computational domain which covers $30 \text{ kpc} \times 30 \text{ kpc} \times 7.5 \text{ kpc}$ of space with $300 \times 300 \times 75$ cells of 3D Cartesian grid, what gives 100 pc of spatial resolution in each direction. the diffusion-advection transport is appended to the set of resistive MHD equations. The CR energy is continuously supplied to the disk by SN remnants. In all models we assume that 10% of 10^{51} erg SN kinetic energy output is converted into the CR energy, while the thermal energy from SN explosions is neglected. Additionally, no initial magnetic field is present but the weak and randomly oriented magnetic field is introduced to the disk in 10% of SN explosions. Following Giacalone & Jokipii (1999) we assume that the CR gas diffuses

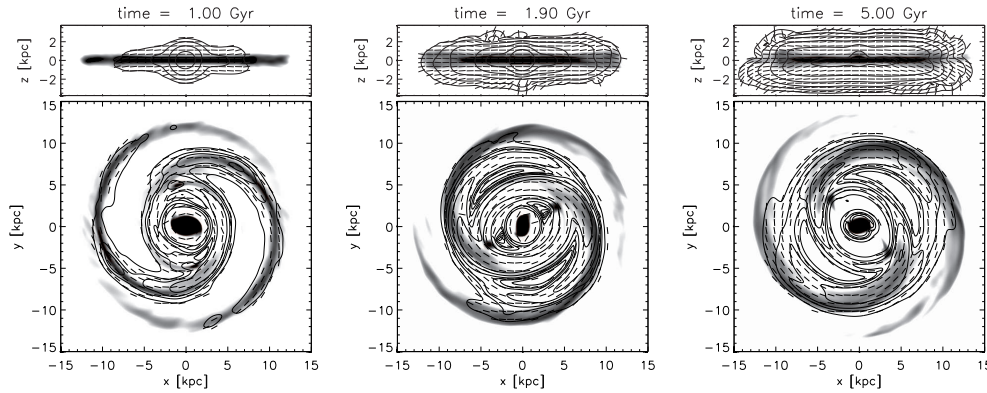


Figure 1. Face-on and edge-on polarization maps at $\lambda = 6.2$ cm for selected times steps. Polarized intensity (contours) and polarization angles (dashes) are superimposed onto column density plots (grey-scale). All maps have been smoothed down to the resolution $40''$. The black color represents the regions with the highest density.

anisotropically along magnetic field lines. In order to allow the topological evolution of magnetic fields we apply a finite uniform magnetic resistivity of the ISM. All numerical simulation have been performed with the aid of the Godunov code (Kowal et al. 2009).

3. Barred galaxy

Figure 1 shows the distributions of polarization angles (vectors) and polarized intensity (contours) superimposed onto the column density maps. On the face-on maps the magnetic field initially follows the gas distribution, as can easily be seen for time $t = 1.0$ Gyr, where the magnetic field strength maxima are aligned with the gaseous ones. However, at later time-steps, the magnetic arms begin to detach themselves from the gaseous spirals and drift into the inter-arm regions. In the edge-on maps the extended structures of the polarization vectors are present. This configuration of the magnetic field vectors bears some resemblance to the extended magnetic halo structures of the edge-on galaxies (so called X-shaped structures).

The face-on and edge-on distribution of the toroidal magnetic field is displayed in Figure 2 (left and middle panels). At $t = 0.5$ Gyr the toroidal magnetic field is mainly disordered as it is introduced to the disk through randomly oriented SN explosions. At later time ($t = 5.1$ Gyr) most of the toroidal magnetic field becomes well ordered. Moreover, we can distinguish regions with negative and positive toroidal magnetic field which form an odd (dipole-type) configuration of the magnetic field with respect to the galactic plane. In Figure 2 (right panel) the exponential growth of the total magnetic energy and the total azimuthal flux due to the CR driven dynamo action in the barred galaxy is shown. At time $t = 5$ Gyr the CR dynamo action saturates and the magnetic field reaches equipartition.

4. Ringed galaxy

CR driven dynamo also works in the case of the ringed galaxy NGC 4736. The exponential growth of the magnetic energy is even faster than in the case of the barred galaxy (Figure 3, right panel). The obtained distribution of the gas density (Figure 3, left panel) as well as the distribution of polarization angles (vectors) and polarized intensity (contours) bear some resemblance to the observation of NGC 4736. To get better

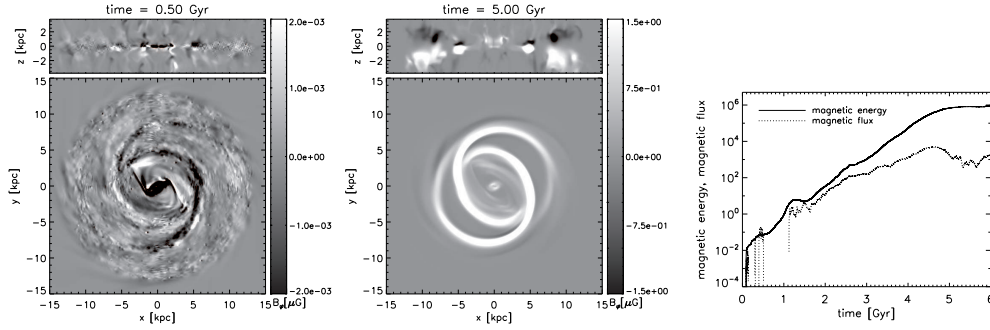


Figure 2. *Left and middle panel:* Distribution of the toroidal magnetic field for selected times steps. The white color represents the regions with the positive toroidal magnetic field, while black with negative. *Right panel:* The time dependence of the total magnetic field energy B^2 (solid line) and the mean B_{ϕ} flux (dashed) calculated for the barred galaxy model.

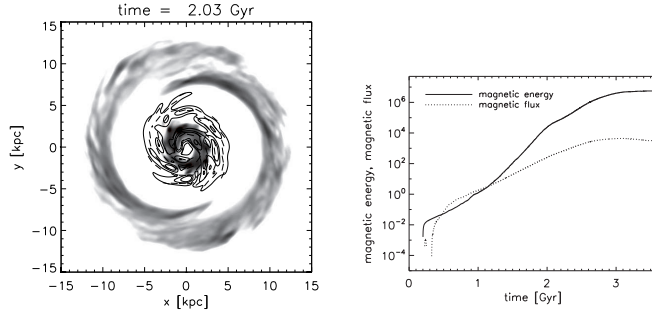


Figure 3. *Left panel:* The face-on polarization map at $\lambda = 6.2$ cm at time $t = 2.03$ Gyr superimposed onto gaseous map. The map has been smoothed to the resolution $40''$. The black color represents the regions with the highest density, white with the smallest. *Right panel:* The time dependence of the total magnetic field energy B^2 (solid line) and the mean B_{ϕ} flux (dashed) calculated for the ringed galaxy model.

results a more sophisticated numerical model of the NGC 4736 is planned. Namely, our model of the ringed galaxy consists of four components: the large and massive halo, the central bulge, the outer disc and the oval distortion. However, following observations of the NGC 4736 this galaxy possesses one more component: the very small bar. Thus, to get better results we have to include the additional small bar in our simulations.

Acknowledgements

This work was supported by Polish Ministry of Science and Higher Education through grants: 92/N-ASTROSIM/2008/0 and 3033/B/H03/2008/35. The computations presented here have been performed on the GALERA supercomputer in TASK Academic Computer Centre in Gdańsk.

References

- Beck, R. *et al.* 2002, *A&A*, 391, 83
 Chyży, K. T. & Buta, R. J., 2008 2008, *ApJ*, 677, L17
 Giacalone, J. & Jokipii, R. J. 1999, *ApJ*, 520, 204
 Hanasz, M., Wóltański, D. & Kowalik, K. 2009, *ApJ*, 706, 155
 Kowal, G., Lazarian, A., Vishniac, E. T. & Otmianowska-Mazur, K. 2009, *ApJ*, 700, 63